SECOND EUROPEAN CONFERENCE ON EARTHQUAKE ENGINEERING
AND SEISMOLOGY, ISTANBUL AUG. 25-29, 2014

# SOURCE SCALING RELATIONS OF SUBDUCTION EARTHQUAKES FOR STRONG GROUND MOTION AND TSUNAMI PREDICTION

Andreas A. SKARLATOUDIS[1] Paul G. SOMERVILLE[2] Hong Kie THIO[3] and Jeffrey R. BAYLESS[4]

## ABSTRACT

The recording on high-resolution, broadband seismic networks of several great interface subduction earthquakes during the last decade provides an excellent opportunity to extend source scaling relations to very large magnitudes and to place constraints on the potential range of source parameters for these events. At present, there is a wide range of uncertainty in the median rupture areas predicted for a given seismic moment by current relationships between magnitude and rupture area for subduction earthquakes. Our goal is to develop an updated set of earthquake source scaling relations that will reduce this current large degree of epistemic uncertainty and improve the accuracy of seismic hazard analysis and the prediction of the strong motion characteristics and tsunamis of future subduction earthquakes. In order to achieve this goal we compiled a database of slip models of interface earthquakes that occurred worldwide with moment magnitudes ranging from **M** 6.75 to **M** 9.1. We characterized the seismic sources based on well-established criteria to estimate the asperity areas and the average slip on the faults and we used these parameters to compute an updated set of magnitude scaling relations of the various characteristics of the fault.

## INTRODUCTION

The ability to predict the ground motions and tsunamis from great subduction earthquakes requires reliable source scaling relations for subduction earthquakes. At present, there is a range of over a factor of 3 in the median rupture areas predicted for a given magnitude by current relationships between magnitude and rupture area for subduction earthquakes. For a given rupture area, there is a range of over 0.5 magnitude unit and a factor of over 5 in seismic moment in the median size of the predicted great earthquakes. We aim to reduce this large epistemic uncertainty in the median values of the scaling relations, while seeking evidence for regional variations in them.

After a long period of quiescence following the 1964 **M** 9.1 Alaska earthquake, several great subduction earthquakes have occurred during the last decade, including the 2001 **M** 8.4 Arequipa, Peru, 2004 **M** 9.1 Sumatra, 2010 **M** 8.8 Chile, and 2011 **M** 9.0 Tohoku earthquakes. The recording of these events on modern digital seismic networks provides an important opportunity to extend the source scaling relations of subduction earthquakes to very large magnitudes, and to place constraints on the potential range of source parameters for these events. Moreover, information about the source characteristics of these recent earthquakes is much more reliable and useful than that of older large earthquakes. This information includes the spatial distribution of slip and slip velocity on the fault,

[1] Seismologist, URS Corp, Los Angeles, andreas.skarlatoudis@urs.com
[2] Principal Seismologist, URS Corp, Los Angeles, paul.somerville@urs.com
[3] Principal Seismologist, URS Corp, Los Angeles, hong.kie.thio@urs.com
[4] Graduate Engineer, URS Corp, Los Angeles, jeff.bayless@urs.com

which is derived from strong motion recordings and in turn is required for the simulation of strong ground motions and tsunamis. Geodetic and tsunami data are also useful for providing constraints on the spatial distribution of slip on the fault.

For predicting strong ground motions, we need to characterize the earthquake source in the frequency band of about 0.1 to 10 Hz or above. For predicting tsunamis, we need to characterize the earthquake source in the frequency band of 0 to 0.01 Hz. Our goal therefore is to develop earthquake source scaling relations for subduction earthquakes over the very broad frequency range of 0 to 10 Hz or above, so that they can be applied to the prediction of both strong ground motions and tsunamis. We distinguish two categories of kinematic source parameters. The first category, consisting of "outer" parameters, includes relationships between seismic moment and rupture length, rupture width, rupture area, and average displacement. These parameters are needed for predicting both ground motions and tsunamis. The second category, consisting of "inner" parameters that describe the heterogeneities of slip and slip velocity (asperities) on the fault rupture surface, includes relations between seismic moment and the spatial and temporal distribution of slip and slip velocity on the fault. The temporal inner parameters are of most importance for the prediction of strong ground motions, which are highly dependent on slip velocity and rupture velocity, but the spatial distribution of slip is also important for tsunami simulation. In the present study we will focus on studying the scaling with seismic moment ($M_o$) of rupture width ($W$), rupture area ($S$), average slip ($D$) and maximum slip ($D_a$) for the "outer" parameters and total asperity area (Sa) for the "inner" parameters.

## COMPILATION OF EARTHQUAKE RUPTURE MODELS DATABASE

We compiled an updated database of interface earthquakes that occurred worldwide in the major subduction zones, with moment magnitudes ranging from **M** 6.75 to **M** 9.1. Information regarding the earthquake location and magnitude, the sources used for the compilation of the database, as well the adopted values of the basic source parameters used in the analysis can be found in Table 1. The locations of these earthquakes are shown in the map of Figure 1.

Table 1. Earthquakes used for source characterization in present study

| A/A | Region | Date | Mw | References | S ($km^2$) | $S_a$ ($km^2$) | D (m) | $D_a$ (m) |
|---|---|---|---|---|---|---|---|---|
| 1 | Central Chile | March 3, 1985 | 8.16 | Mendoza et al. (1994) | 34425 | 9675 | 1.92 | 1.75 |
| 2 | Michoacan, Mexico | September 19, 1985 | 8.01 | Mendoza and Hartzell (1989) | 25020 | 5004 | 1.40 | 2.95 |
| 3 | Sanrikuki, Japan | December 28, 1994 | 7.70 | Nagai et al. (2001) | 15400 | 2600 | 0.71 | 1.95 |
| 4 | Colima, Mexico | October 9, 1995 | 7.96 | Mendoza and Hartzell (1999) | 17000 | 2800 | 1.18 | 2.80 |
| 5 | Nazca Ridge, Peru | November 12, 1996 | 8.06 | Spence et al. (1999) | 36000 | 9072 | 0.77 | 1.53 |
| 6 | Colima, Mexico | January 22, 2003 | 7.50 | Yagi et al. (2004) | 5950 | 1350 | 0.61 | 1.30 |
| 7 | Tokachi-oki, Japan | September 25, 2003 | 8.16 | Yagi (2004) | 22100 | 5600 | 1.46 | 3.15 |
| 8 | Giant Sumatra Earthquake (Indonesia) | December 26, 2004 | 8.89 | Ammon et al. (2005) | 265237 | 27571 | 3.90 | 6.70 |
| 9 | Honshu, Japan | August 16, 2005 | 7.50 | Shao and Ji (UCSB, Honshu 2005) | 3584 | 960 | 0.15 | 0.70 |
| 10 | Sumatra | March 28, 2005 | 8.68 | Shao and Ji (UCSB, Sumatra 2005) | 86400 | 27200 | 2.56 | 5.45 |
| 11 | Kuril Islands | November 15, 2006 | 8.30 | Ji (UCSB, Kuril 2006) | 35750 | 10000 | 1.69 | 5.10 |
| 12 | Solomon Islands | April 1, 2007 | 8.10 | Ji (UCSB, Solomon Islands 2007) | 21600 | 6600 | 1.47 | 2.70 |
| 13 | Benkulu, Indonesia | September 12, 2007 | 8.40 | Ji (UCSB, Benkulu 2007) | 73140 | 28331 | 0.90 | 1.85 |
| 14 | Pagai, Indonesia | September 12, 2007 | 7.90 | Ji and Zeng (Pagai 2007) ) | 21875 | 6500 | 0.55 | 1.47 |

| | | | | | | | | |
|---|---|---|---|---|---|---|---|---|
| 15 | Tocopilla, Chile | November 14, 2007 | 7.70 | Sladen (Caltech, Tocopilla 2007) | 18954 | 7695 | 0.88 | 1.75 |
| 16 | Pisco, Peru | August 15, 2007 | 8.00 | Ji and Zeng (Peru 2007) | 20736 | 5508 | 1.63 | 3.80 |
| 17 | Papua | January 3, 2009 | 7.60 | Hayes (NEIC, Papua 2009) | 11520 | 1680 | 0.59 | 2.00 |
| 18 | Vanuatu | October 7, 2009 | 7.60 | Sladen (Caltech, Vanuatu 2009) | 4200 | 1680 | 0.87 | 2.05 |
| 19 | Fiordland, New Zealand | July 15, 2009 | 7.60 | Hayes (NEIC, New Zealand 2009) | 10752 | 2560 | 0.63 | 2.60 |
| 20 | Samoa | September 29, 2009 | 8.00 | Hayes (NEIC, Samoa 2009) | 7243 | 1983 | 3.33 | 8.98 |
| 21 | Maule, Chile | February 27, 2010 | 8.80 | Lorito et al. (2011) | 115000 | 31875 | 4.13 | 9.00 |
| 22 | Tohoku-Oki, Japan | March 11, 2011 | 9.09 | Yokota et al., (2011) | 81000 | 18900 | 10.51 | 22.97 |
| 23 | Costa Rica | September 5, 2012 | 7.57 | Hayes (NEIC, Costa Rica 2012) | 18000 | 3520 | 0.29 | 0.95 |
| 24 | Masset,Canada | October 28, 2012 | 7.72 | Shao and Ji (UCSB, Masset 2012) | 4800 | 1440 | 1.57 | 4.80 |
| 25 | East of Sulangan, Philippines | August 31, 2012 | 7.59 | Hayes (USGS, Philippines 2012) | 4608 | 1440 | 0.42 | 1.90 |
| 26 | Near Coast Of Guerrero, Mexico | March 3, 2012 | 7.40 | Wei (Caltech, Oaxaca 2012) | 4125 | 1050 | 0.41 | 0.20 |
| 27 | Peru | October 3, 1974 | 8.02 | Somerville et al. (2002) | 28000 | 6066 | 1.30 | 2.19 |
| 28 | Hokkaido Nansei | November 12, 1993 | 7.65 | Mendoza and Fukuyama (1996) | 14000 | 2300 | 0.64 | 1.64 |
| 29 | Zihuatanejo | September 21, 1985 | 7.39 | Somerville et al. (2002) | 3150 | 1350 | 1.02 | 1.54 |
| 30 | Playa Azul | October 25, 1981 | 7.20 | Somerville et al. (2002) | 2700 | 400 | 0.74 | 2.37 |
| 31 | Peru | November 9, 1974 | 7.12 | Somerville et al. (2002) | 3000 | 600 | 0.54 | 1.16 |
| 32 | Arequipa | June 23, 2001 | 8.35 | Somerville et al. (2003) | 80000 | 20800 | 1.22 | 2.48 |
| 33 | Alaska | March 27, 1964 | 9.18 | Ichinose et al., (2007) | 225000 | 30000 | 4.00 | 11.30 |
| 34 | Chile | May 22, 1960 | 9.20 | Fujii and Satake (2013) | 135000 | 40000 | 10.6 | - |
| 35 | Aleutian | March 9, 1957 | 8.69 | Johnson et al. (1994) | 93750 | 30000 | 3.1 | - |
| 36 | Kamchatka | November 4, 1952 | 8.75 | Johnson and Satake, (1999) | 70000 | 20000 | 5.5 | - |
| 37 | Hyuga-nada, Japan | December 2, 1996 | 6.75 | Yagi et al. (1999) | 179 | 153.5 | 0.42 | 0.92 |
| 38 | Sanriku-haruka-oki, Japan | December 28, 1994 | 7.73 | Nagai et al. (2001) | 2800 | 2800 | 0.71 | 1.93 |
| 39 | Nihonkai-chubu, Japan | May 26, 1983 | 7.62 | Fukuyama and Irikura (1986) | - | - | 3.17 | - |
| 40 | Hyuga-nada, Japan | April 1, 1968 | 7.57 | Yagi et al. (1998) | 1377 | 1053 | 1.32 | 2.9 |
| 41 | Tokachi-oki, Japan | May 16, 1968 | 8.33 | Nagai et al.(2001) | 6800 | 5600 | 2.31 | 5.49 |
| 42 | Nankai, Japan | December 21, 1946 | 8.36 | Satake (1993) | - | - | 0.84 | - |
| 43 | Tonankai, Japan | December 7, 1944 | 8.22 | Ichinose et al.(2003) | 4000 | 4800 | 1.05 | 1.78 |
| 44 | Kanto , Japan | September 1, 1923 | 7.89 | Wald and Somerville (1995) | 2340 | 2210 | 2.54 | 5.6 |

The majority of the finite-fault rupture models of the earthquakes in Table 1 was available from the online database "Finite Source Rupture Model Database" (http://equake-rc.info/SRCMOD/). To characterize asperities in these cases the definition given in Somerville et al. (1999) was followed: "***An***

***asperity is initially defined to enclose fault elements whose slip is 1.5 or more times larger than the average slip over the fault and was subdivided if any row or column has an average slip less than 1.5 times the average slip"***. When the original slip model was not available in the database we used the source characterization parameters reported in the literature.

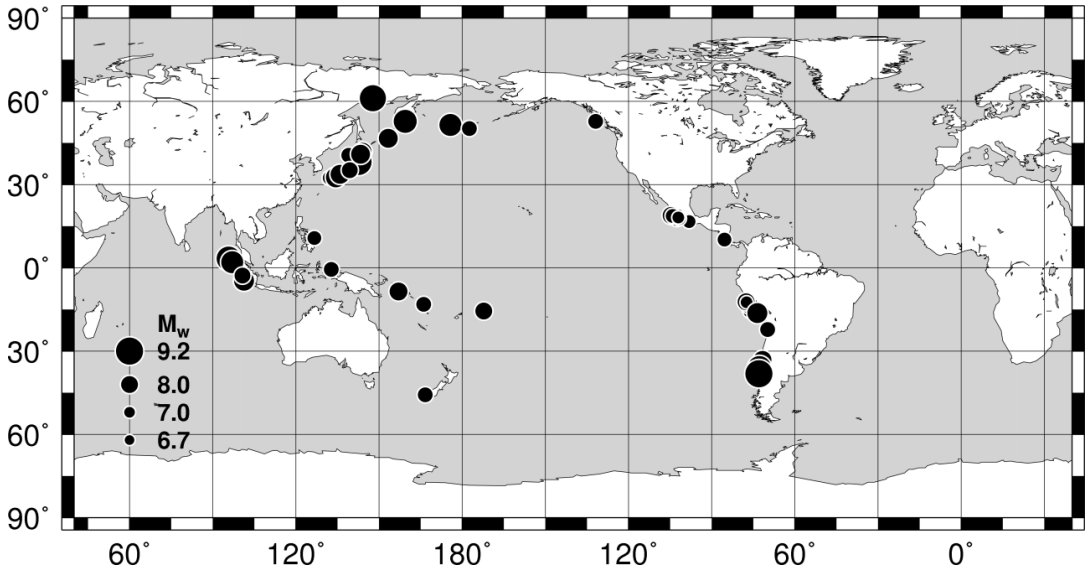


Figure 1. Map showing the locations of the earthquakes listed in Table 1.

We evaluated all available rupture models of each earthquake in order to understand the uncertainty in the slip model inversion process and to identify the best constrained features of the rupture models of these earthquakes. When an earthquake had more than one available rupture model we selected the one that was based on the largest number of strong motion or teleseismic data for use in our analysis.

## DEVELOP OF SOURCE SCALING RELATIONSHIPS

We used the updated database of finite-fault rupture models that we compiled to produce scaling relations of the various source parameters. For the regressions we used a maximum likelihood analysis (Draper and Smith, 1981) with an optimization procedure based on the weighted least-squares method using the singular value decomposition method (Lanczos, 1961). Uncertainty in both the seismic moment and source parameter estimates was taken into account by assuming a10% variability in the seismic moment values and a 20% variability to the source parameter estimates. Each equation was weighted with the total uncertainty which was computed using error propagation theory.

We fit the data using self-similar relationships with a constrained slope. For the rupture area ($S$) and total asperity area ($S_a$) (km$^2$) the slope is constrained to 2/3 ($S = CM_0^{2/3}$), while for the average slip ($D$) and maximum slip ($D_{max}$) (m) the slope is constrained to 1/3 ($D = CM_0^{1/3}$). The coefficients and the standard deviations from various studies estimated for the self-similar functional forms are listed in Table 2. Somerville et al. (2002) used the CGS system of units for $M_0$ (dyn.cm) and D (cm).

Table 2. Regression coefficients and their standard deviations from various studies assuming self-similarity.

| | $M_o$-S | | $M_o$-D | | $M_o$-$S_a$ | | $M_o$-$D_{max}$ | |
|---|---|---|---|---|---|---|---|---|
| | c | σ | c | σ | C | σ | c | σ |
| Present Study | 1.17E-10 | 1.17 | 1.30E-07 | 1.19 | 4.16E-11 | 1.19 | 5.02E-07 | 1.23 |
| Murotani et al. (2013) | 1.34E-10 | 1.54 | 1.66E-07 | 1.64 | 2.81E-11 | 1.72 | - | - |
| Murotani et al. (2008) | 1.48E-10 | 1.61 | 1.48E-07 | 1.72 | 2.89E-11 | 1.78 | - | - |
| Somerville et al. (2002) | 5.20E-15 | - | 5.30E-08 | - | 1.21E-15 | - | - | - |

In Figures 2 and 3 the derived relations for $S$ and $S_a$ (black solid lines) are plotted together with the data used in the analysis (different symbols for the various data sources). The shaded area represents the $\pm 1$ standard deviation. For the rupture area, the mean values computed in this study are very similar (within $\pm 1$ standard deviation) of those reported in Murotani et al. (2008; 2013) (magenta solid and dashed lines, respectively). The comparison of the present study results with those of Somerville et al. (2002) (light blue line) indicates smaller areas for the same seismic moment in the new relationships. Figure 3 shows that present study results estimate larger combined asperity areas for the same seismic moment than those from Murotani et al. (2008; 2013) and Somerville et al. (2002).

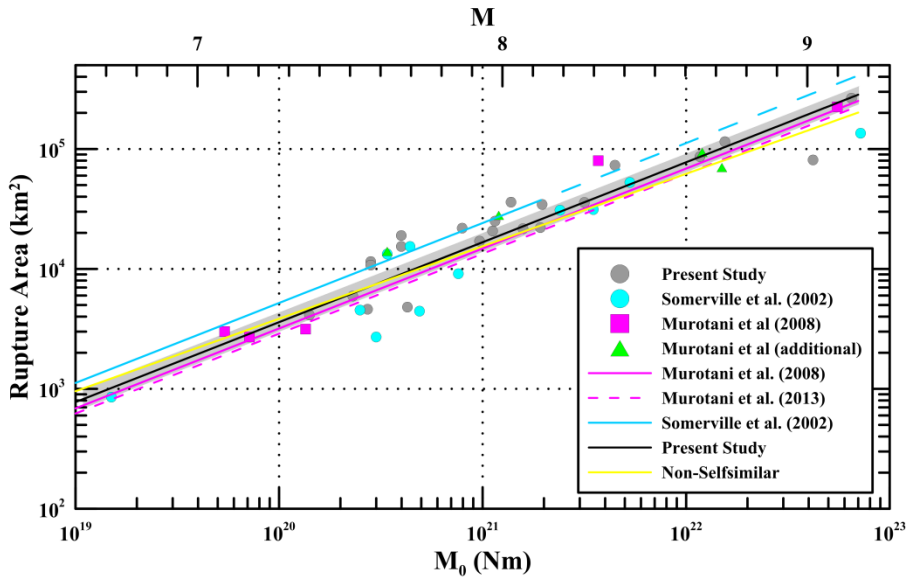


Figure 2. Scaling relations of rupture area plotted together with data from various studies with respect to seismic moment. The shaded area indicates the standard deviation of 1.17.

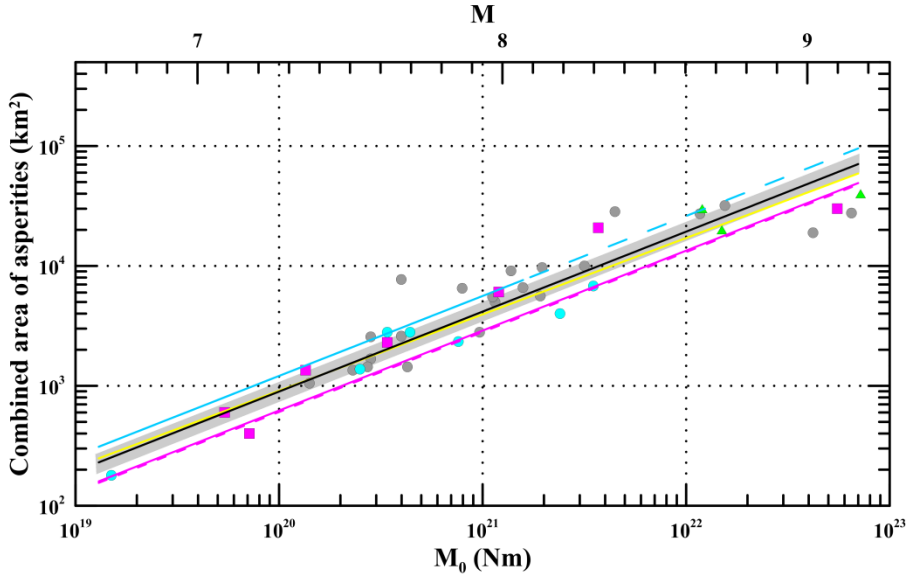


Figure 3. Scaling relations of combined area of asperities plotted together with data from various studies with respect to seismic moment. The shaded area indicates the standard deviation of 1.19.

The derived relations for the average and maximum slip are shown in Figures 4 and 5. The colors and symbols used in these plots are the same as the ones used in the previous figures. For the average slip, the mean values computed in this study are very similar to those estimated both in Murotani et al. (2008; 2013) and Somerville et al. (2002). The results for the maximum slip scaling are

characterized by large scatter in the data in the intermediate range of seismic moment values as well as by the lack of data at larger magnitudes, since only two values drive the regressions results for **M**≥9. This is also reflected in the standard deviation, which is the largest of all the standard deviation values computed for the source parameters studied.

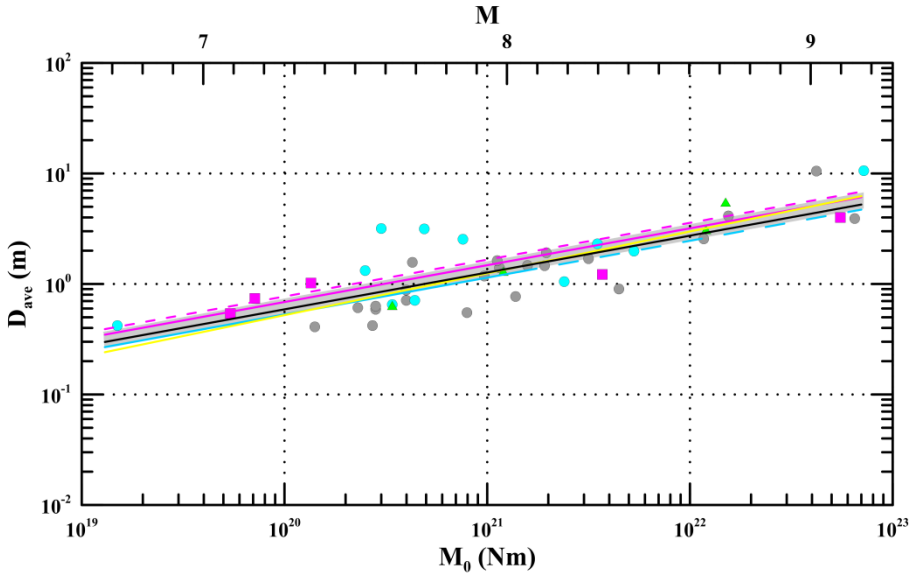


Figure 4. Scaling relations of average slip plotted together with data from various studies with respect to seismic moment. The shaded area indicates the standard deviation of 1.19.

We assumed self-similar scaling laws in performing the regression analysis. However, there are studies (e.g. Strasser et al., 2010; Papazachos et al., 2004) that reveal a departure from self-similar scaling of the total rupture area and slip of the fault. In order to investigate the sensitivity of our results to the different functional forms, we also fit the data to non-self-similar relationships. The scaling of fault width with seismic moment assuming a non-self-similar functional form was also investigated. The coefficients and the standard deviations estimated from these regressions are listed in Table 3.

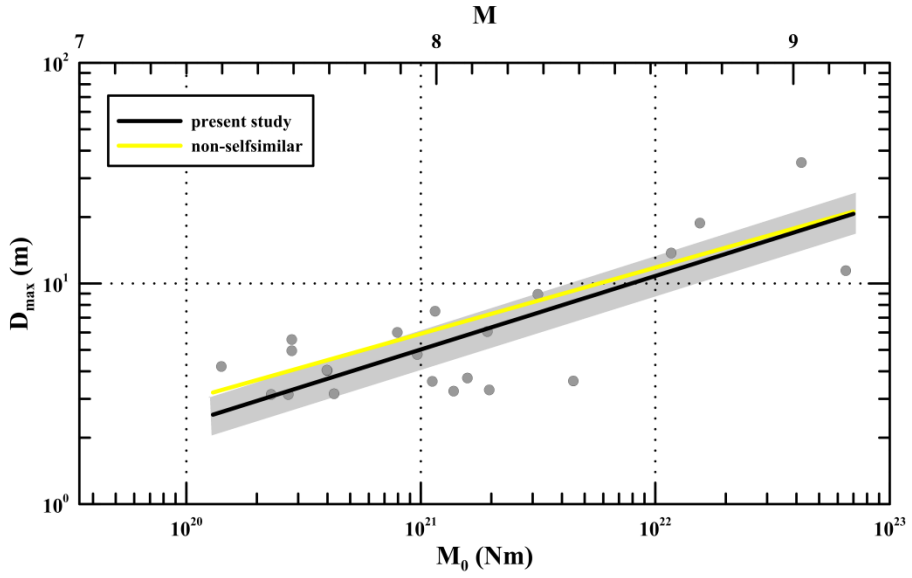


Figure 5. Scaling relation of maximum slip with respect to seismic moment. Self-similar and non-self-similar fits to the data are shown with different colors.

In Figures 2 through 5 the regression results for the non-self-similar functional forms are shown with the yellow curves. The comparison with the black curves (self-similar functional forms) does not exhibit substantial differences. Moreover, the standard deviations listed in Tables 3 and 4 have very

similar values. Since the differences are not large, we prefer to retain the simplicity of using the self-similar relations.

Table 3. Form of the various scaling relations, regression coefficients and their standard deviations.

| Functional Form | $c_1$ | $c_2$ | σ |
|---|---|---|---|
| $A = c_1 \times M_o^{c2}$ | 7.60E-10 | 1.89 | 1.17 |
| $D = c_1 \times M_o^{c2}$ | 9.52E-07 | 1.40 | 1.19 |
| $A_a = c_1 \times M_o^{c2}$ | 4.81E-10 | 1.85 | 1.19 |
| $W = c_1 \times M_o^{c2}$ | 7.58E-03 | 1.22 | 1.11 |
| $D_{max} = c_1 \times M_o^{c2}$ | 2.95E-06 | 1.35 | 1.23 |

In Figure 6 the scaling of fault width with respect to seismic moment is presented. For magnitudes **M**>9 the saturation of the fault width is suggested, but the limited number of data prevents better constraining the fit.

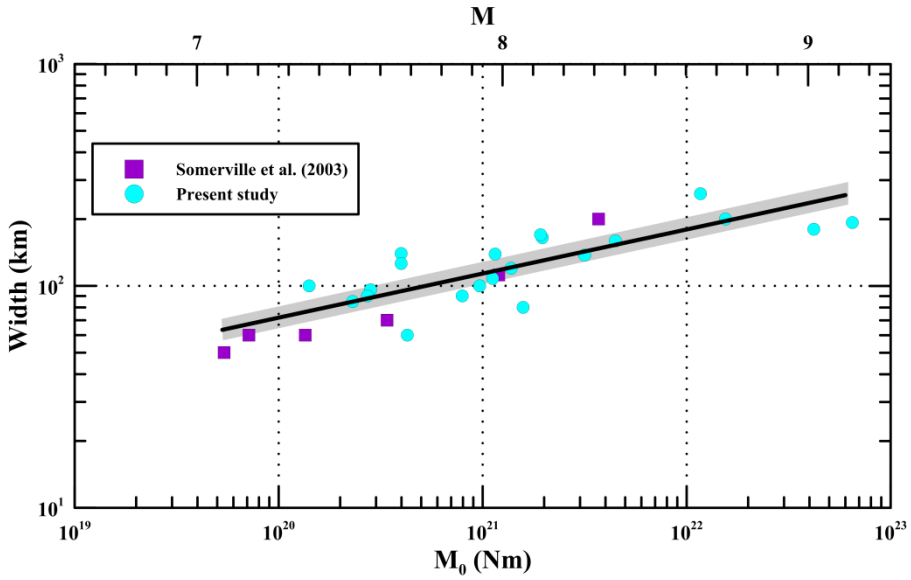


Figure 6. Scaling relation of fault width with respect to seismic moment. The shaded area indicates the standard deviation of 1.11.

The differences in rupture areas between subduction and crustal earthquakes were originally identified by Somerville et al. (1999) and later by several other studies (e.g. Strasser et al., 2010; Murotani et al., 2008; 2013, Papazachos et al., 2004). Somerville et al. (1999) reported that on average, subduction earthquakes have rupture areas that are two or more times larger than those of crustal earthquakes having the same seismic moment. In order to test this assumption with our dataset, we compared the scaling coefficients of Table 2 with the corresponding ones reported in Somerville et al. (1999) for crustal earthquakes. We found that on average, the rupture areas of subduction earthquakes are ~1.7 times larger and the average slip is ~0.4 times as large as those of crustal earthquakes having the same seismic moment.

## CONCLUSIONS

We compiled an updated database of interface earthquakes that occurred worldwide in the major subduction zones with moment magnitudes ranging from **M** 6.75 to **M** 9.1. We evaluated all available rupture models for each earthquake and selected the ones that were based on the largest number of strong motion or teleseismic data. In order to estimate the various source parameters we characterized the asperities for the original slip models based on a well-established methodology (Somerville et al., 1999).

We studied the scaling with seismic moment of rupture width, rupture area, total asperity area and of the average and maximum slip. In all cases the standard deviations are considerably smaller than the values estimated by Murotani et al. (2008; 2013) as a result of the larger number of records used in the regressions. Another factor that might have contributed to the smaller standard deviations is that we did not use more than one model of the same earthquake in the regression analysis. In cases where we had multiple source models for a single earthquake, we used judgment to select the most representative one based on various criteria such as the number and type of data used in deriving the model. Despite the much larger number of available data including the ones from the latest mega-thrust earthquakes, there are still few points to constrain the behavior of the scaling curves at high magnitudes (**M**>9.0) (e.g. fault width, Figure 6).

Although the goal to reduce the epistemic uncertainty was achieved, comparison of the available scaling models of rupture area for both self-similar and non-self-similar functional forms presented in Figure 7 points out that there are still large differences between the models, and additional work is needed in order to investigate the source of this difference between the various studies.

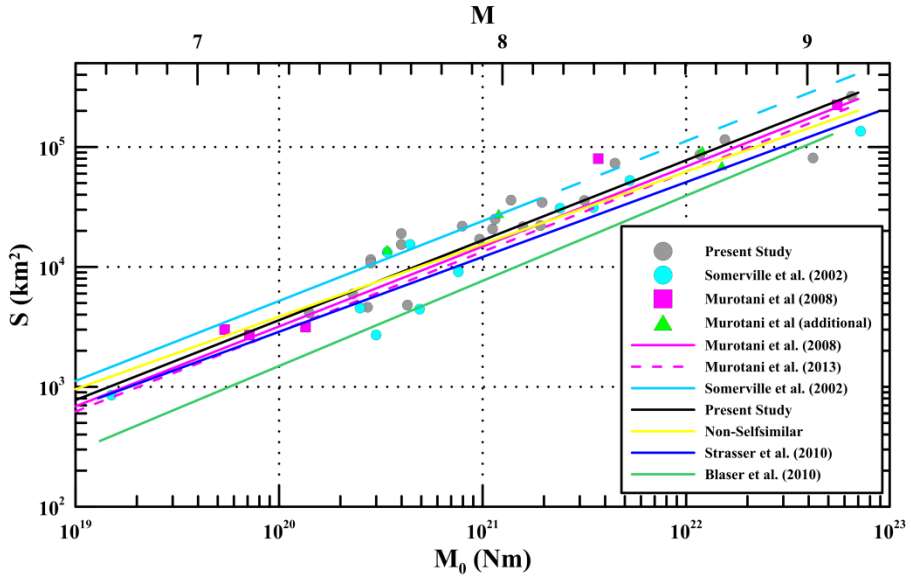


Figure 7. Scaling relations of rupture area plotted together with data from various studies with respect to seismic moment.

The results from our regression analysis do not support in a definite way any of the two functional forms used to fit the data, since in most of the cases median values were very similar. However, since the differences are not large, we prefer to retain the simplicity of using the self-similar relations as found by some of the previous studies (Murotani et al., 2013; 2008, Somerville et al., 2002).

## ACKNOWLEDGMENTS

Research on the Maule and Tohoku earthquakes supported by the U.S. Geological Survey (USGS), Department of the Interior, under USGS award number (Paul Somerville, G13AP00028). The views and conclusions contained in this document are those of the authors and should not be interpreted as necessarily representing the official policies, either expressed or implied, of the U.S. Government. Some plots were created using the Generic Mapping Tools version 4.2.1 (Wessel and Smith, 1998).

## REFERENCES


Ammon CJ, J Chen, HK Thio, D Robinson, S Ni, V Hjorleifsdottir, H Kanamori, T Lay, S Das, D Helmberger, G Ichinose, J Polet, and D Wald (2005). Rupture process of the great 2004 Sumatra-Andaman earthquake, *Science*, 308, 1133-1139.

Blaser L, F Krüger, M Ohrnberger, and F Scherbaum (2010). Scaling relations of earthquake source parameter estimates with special focus on subduction environment, *Bull. Seismol. Soc. Am.*, 100, 2914–2926, doi:10.1785/0120100111.

Draper NR, and H Smith (1981). Applied Regression Analysis, Second Ed., Wiley, New York, 709 pp.

Fukuyama E and K Irikura (1986). Rupture process of the 1983 Japan Sea (Akita-Oki) earthquake using a waveform inversion method, *Bull. Seismol. Soc. Am.*, 76, 1623–1640.

Fujii Y, and K Satake (2013). Slip distribution and seismic moment of the 2010 and 1960 Chilean earthquakes inferred from tsunami waveforms and coastal geodetic data, *Pure Appl. Geophys.*, 170, 1493–1509.

Hayes G (NEIC, Papua 2009). Preliminary Result of the Jan 3, 2009 Mw 7.6 Papua Earthquake, http://earthquake.usgs.gov/earthquakes/eqinthenews/2009/us2009bjbn/finite_fault.php,,last accessed August 29, 2013.

Hayes G (NEIC, New Zealand 2009). Preliminary Result of the July 15, 2009 Mw 7.6 Fiordland Earthquake, http://earthquake.usgs.gov/earthquakes/eqinthenews/2009/us2009jcap/finite_fault.php, last accessed August 19, 2013.

Hayes G (NEIC,Costa Rica 2012). Preliminary Result of the Sep 5, 2012 Mw 7.6 Costa Rica Earthquake, http://earthquake.usgs.gov/earthquakes/eqinthenews/2012/usc000cfsd/finite_fault.php,last accessed August 21, 2013.

Hayes G (NEIC,Samoa 2009). Preliminary Result of the Sep 29, 2009 Mw 8.0 Samoa Earthquake, http://earthquake.usgs.gov/earthquakes/eqinthenews/2009/us2009mdbi/finite_fault.php,last accessed August 29, 2013.

Hayes G (USGS, Philippines 2012). Preliminary Result of the Aug 31, 2012 Mw 7.6 earthquake east of Sulangan,Philippines,http://earthquake.usgs.gov/earthquakes/eqinthenews/2012/usc000cc5m/finite_fault.php, last accessed August 21, 2013.

Ichinose GA, HK Thio, PG Somerville, T Sato, and T Ishii (2003). Rupture process of the 1944 Tonankai earthquake (*M*s 8.1) from the inversion of teleseismic and regional seismograms, *J. Geophys. Res.*, 108, 2497, doi:10.1029/2003JB002393.

Ichinose G, P Somerville, HK Thio, R Graves, and D O'Connell (2007). Rupture process of the 1964 Prince William Sound, Alaska, earthquake from the combined inversion of seismic, tsunami, and geodetic data, *J. Geophys. Res.*, 112, doi 10.1029/2006JB004728.

Ji C and Y Zeng (Sumatra 2005). Preliminary Result of the Sep 12, 2007 Mw 7.9 Kepulauan Earthquake,http://earthquake.usgs.gov/earthquakes/eqinthenews/2007/us2007hec6/finite_fault.php, last accessed August 14, 2013.

Ji C (UCSB,Kuril 2006). Rupture process of the 2006 Nov 15 Magnitude 8.3 - KURIL Island Earthquake(Revised),http://earthquake.usgs.gov/earthquakes/eqinthenews/2006/usvcam/finite_fault.php,last accessed September 5, 2013.

Ji C and Y Zeng (Peru 2007). Preliminary Result of the Aug 15, 2007 Mw 8.0 Coast of Central Peru Earthquake, ttp://earthquake.usgs.gov/earthquakes/eqinthenews/2007/us2007gbcv/finite_fault.php, last accessed August 21, 2013.

Ji C (UCSB, Benkulu 2007). Rupture Process of the Sep 12, 2007 Mw 8.4 Sumatra Earthquake: Phase II, http://www.geol.ucsb.edu/faculty/ji/big_earthquakes/2007/09/sumatra_seismic.html, Last accessed August 12, 2013.

Ji C (UCSB,Solomon Islands 2007). Rupture process of the 2007 April 1, Magnitude 8.1, Solomon IslandsEarthquake,http://earthquake.usgs.gov/earthquakes/eqinthenews/2007/us2007aqbk/finite_fault.php,last accessed August 27, 2013.

Johnson JM, Y Tanioka, LJ Ruff, K Satake, H Kanamori, and LR Sykes (1994). The 1957 great Aleutian earthquake, *Pure Appl. Geophys.*, 142, 3–28.

Johnson JM, and K Satake (1999). Asperity distribution of the 1952 great Kamchatka earthquake and its relation to future earthquake potential in Kamchatka, *Pure Appl. Geophys.*, 154, 541–553.

Lanczos C (1961). Linear Differential Operators, D. Van Nostrand, Princeton, New Jersey, 564 pp.

Lorito S, F Romano, S Atzori, X Tong, A Avallone, J McCloskey, M Cocco, E Boschi, and A Piatanesi (2011). Limited overlap between the seismic gap and coseismic slip of the great 2010 Chile earthquake, *Nature Geoscience*, 4, 173–177, doi:10.1038/ngeo1073.

Mendoza C and E Fukuyama (1996). The July 12, 1993, Hokkaido Nansei- Oki, Japan, earthquake: Coseismic slip pattern from strong-motion and teleseismic recordings, *J. Geophys. Res.*, 101, 791–801.

Mendoza C and S Hartzell (1989). Slip distribution of the 19 September 1985 Michoacan, Mexico, earthquake: near-source and teleseismic constraints, *Bull. Seism. Soc. Am*., 79, 655- 669.

Mendoza C, and S Hartzell (1999). Fault-slip distribution of the 1995 Colima-Jalisco, Mexico, earthquake. *Bull. Seis. Soc. Am*, 89, 1338-1344.

Mendoza C, S Hartzell and T Monfret (1994). Wide-band analysis of the 3 March 1985 central Chile earthquake: overall source process and rupture history, *Bull. Seism. Soc. Am*., 84, 269-283.

Murotani S, H Miyake, and K Koketsu (2008). Scaling of characterized slip models for plate-boundary earthquakes, *Earth Planets Space*, 60, 987–991.

Murotani S, K Satake and Y Fujii (2013). Scaling relations of seismic moment, rupture area, average slip, and asperity size for M~9 subduction-zone earthquakes, *Geoph. Res. Lett.*, 40, 1-5.

Nagai R, M Kikuchi, and Y Yamanaka (2001). Comparative study on the source processes of recurrent large *earthquakes* in Sanriku-oki region: the 1968 Tokachi-oki earthquake and the 1994 Sanriku-oki earthquake, *Zisin*, 54, 267–280 (in Japanese with English abstract).

Papazachos BC, EM Scordilis, DG Panagiotopoulos, CB Papazachos and GF Karakaisis (2004). Global relations between seismic fault parameters and moment magnitudes of earthquakes. *Bulletin of the Geological Society of Greece*, 36, 1482-1489.

Satake K (1993). Depth distribution of coseismic slip along the Nankai trough, Japan, from joint inversion of *geodetic* and tsunami data, *J. Geophys. Res.*, 98, 4553–4565.

Shao G and C Ji (UCSB, Masset 2012). Preliminary Result of the Oct 28, 2012 Mw 7.72 Canada Earthquake, http://www.geol.ucsb.edu/faculty/ji/big_earthquakes/2012/10/canada.html, last accessed August 20, 2013.

Shao G and C Ji (UCSB, Honshu 2005). Preliminary Result of the Aug 16, 2005 Mw 7.19 honshu Earthquake, http://www.geol.ucsb.edu/faculty/ji/big_earthquakes/2005/08/smooth/honshu.html, last accessed August 22, 2013.

Shao G and C Ji (UCSB, Sumatra 2005). Preliminary Result of the Mar 28, 2005 Mw 8.68 nais Earthquake, http://www.geol.ucsb.edu/faculty/ji/big_earthquakes/2005/03/smooth/nias.html, last accessed August 25, 2013.

Sladen A (Caltech, Tocopilla 2007). Preliminary Result 11/14/2007 (Mw 7.7), Tocopilla Earthquake, Chile. Source Models of Large Earthquakes. http://www.tectonics.caltech.edu/slip_history/2007_tocopilla/tocopilla.html, last accessed July 1, 2013.

Sladen A (Caltech, Vanuatu 2009). Preliminary Result 10/07/2009 (Mw 7.6), Vanuatu. Source Models of Large Earthquakes. http://www.tectonics.caltech.edu/slip_history/2009_vanuatu/index.html, last accessed July 1, 2013.

Somerville PG, HK Thio, G Ichinose, N Collins, A Pitarka, and R Graves (2003). Earthquake source and ground motion characteristics of the June 23, 2001 Mw 8.4 Arequipa, Peru, earthquake, *Seismol. Res. Lett.* 74, 223.

Somerville PG, K Irikura, R Graves, S Sawada, D Wald, N Abrahamson, Y Iwasaki, T Kagawa, N Smith, and A Kowada (1999). Characterizing crustal earthquake slip models for the prediction of strong ground motion, *Seismol. Res. Lett.* 70, 59–80.

Somerville PG, T Sato, T Ishii, NF Collins, K Dan and H Fujiwara (2002). Characterizing heterogeneous slip models for the large subduction earthquakes for strong ground motion prediction. *Proc. 11th Japan Earthquake Engineering Symposium*, 163-166 (in Japanese with English abstract).

Spence W, C Mendoza, ER Engdahl, GL Choy, and E Norabuena (1999). Seismic subduction of the Nazca Ridge as shown by the 1996-97 Peru earthquakes, *Pure and Applied Geophysics*, 154, 753-776.

Strasser FO, MC Arango, and JJ Bommer (2010). Scaling of the source dimensions of interface and intraslab subduction-zone earthquakes with moment magnitude, *Seismol. Res. Lett.* 81, 941–950.

Wald DJ and PG Somerville (1995). Variable-slip rupture model of the great 1923 Kanto, Japan, earthquake: Geodetic and body-waveform analysis, *Bull. Seismol. Soc. Am.*, **85**, 159–177.

Wei S (Caltech, Oaxaca 2012). March/20/2012 (Mw 7.4), OAXACA, Mexico. Source Models of Large Earthquakes. http://www.tectonics.caltech.edu/slip_history/2012_Mexico/index.html, last accessed July 1, 2013.

Wessel P, and HF Smith (1998). New, improved version of the generic mapping tools released, Eos Transactions AGU 79, 579.

Yagi Y, M Kikuchi, S Yoshida, and Y Yamanaka (1998). Source process of the Hyuga-nada earthquake of April 1, 1968 (*M*JMA 7.5), and its relationship to the subsequent seismicity, *Zisin*, 51, 139–148 (in Japanese with English abstract).

Yagi Y (2004). Source rupture process of the 2003 Tokachi-oki earthquake determined by joint inversion of teleseismic body wave and ground motion data, *Earth Planets Space*, 56, 311–316.

Yagi Y, T Mikurno, J Pacheco, and G Reyes (2004). Source rupture process of the Tecoman, Colima, Mexico earthquake of 22 January 2003, determined by joint inversion of teleseismic body-wave and near-source data, *Bull. Seis. Soc. Am*, 94, 1795-1807.

Yagi Y, M Kikuchi, S Yoshida and T Sagiya (1999). Comparison of the coseismic rupture with the aftershock distribution in the Hyuga-nada earthquakes of 1996, *Geophys. Res. Lett.*, 26, 3161–3164.

Yokota Y, K Koketsu, Y Fujii, K Satake, S Sakai, M Shinohara, and T Kanazawa (2011). Joint inversion of strong motion, teleseismic, geodetic, and tsunami datasets for the rupture process of the 2011 Tohoku earthquake, *Geophys. Res. Lett.*, 38, doi:10.1029/2011GL050098.